A LAGROBO strategy to fit potential energy surfaces: the OH + HCl reaction

ARTICLE *in* CHEMICAL PHYSICS LETTERS · JULY 2002

Impact Factor: 1.9 · DOI: 10.1016/S0009-2614(02)00835-7

4 AUTHORS, INCLUDING:

Aurelio Rodríguez-López
Centro de Supercomputación de Galicia
9 PUBLICATIONS **114** CITATIONS
SEE PROFILE

Ernesto Garcia
Universidad del País Vasco / Euskal He…
93 PUBLICATIONS **1,138** CITATIONS
SEE PROFILE

Antonio Laganà
Università degli Studi di Perugia
162 PUBLICATIONS **1,051** CITATIONS
SEE PROFILE

10 July 2002

ELSEVIER

Chemical Physics Letters 360 (2002) 304–312

CHEMICAL PHYSICS LETTERS

www.elsevier.com/locate/cplett

A LAGROBO strategy to fit potential energy surfaces: the OH + HCl reaction

Aurelio Rodriguez [a], Ernesto Garcia [a], M. Luz Hernández [b], Antonio Laganà [c,*]

[a] *Departamento de Química Física, Universidad del País Vasco, 01006 Vitoria, Spain*
[b] *Departamento de Física de la Atmósfera, Universidad de Salamanca, 37008 Salamanca, Spain*
[c] *Dipartimento di Chimica, Università di Perugia, 06123 Perugia, Italy*

Received 14 March 2002; in final form 15 May 2002

Abstract

The LAGROBO functional formulation of the interaction for four atom reactions is revisited and a strategy to fit the potential energy surface of the OH + HCl reaction to measured rate coefficients is discussed. The flexibility of the LAGROBO functional has allowed to keep the changes highly localized and to estimate the effect of varying the height of the barrier to reaction on the value of the related rate coefficients. An interesting agreement with the low temperature data is also found.

1. Introduction

A quantitative information on the global reactive OH + HCl process is provided by some kinetic experiments whose most important outcome is a set of reaction coefficients. Most of the measurements were performed in the years 1984–1985 for temperatures ranging from 200 to 1000 K. Measured rates were fitted using Arrhenius-like expressions [1–4]. More recently other measurements were performed [5,6]. On the basis of these data, the IUPAC Subcommittee on Gas Kinetic Data Evaluation for Atmospheric Chemistry has published some recommended values [7]. However, for reasons that will become clearer later on, we point out here that values of the rate coefficients reported in [5] deviate from the low temperature extrapolation of recommended data.

On the theoretical side, the first dynamical investigation of the OH + HCl reaction using an *ad hoc* potential energy surface (PES) was worked out by Clary, Nyman and Hernandez (CNH) in 1994 [8]. The CNH PES makes use of a simplified formulation of the interaction that combines the LEPS functional describing the interaction of the O + HCl → OH + Cl process with that of the water molecule of [9]. The CNH PES has only one adjustable parameter that was optimized to reproduce the height (7.18 kcal mol^{-1}) of the transition state estimated by performing ab initio UMP2 calculations. The geometry of the transition state is coplanar with a *trans* configuration and an

* Corresponding author. Fax: +39-075-5855606.
E-mail addresses: lag@unipg.it, lag@impact.dyn.unipg.it (A. Laganà).

0009-2614/02/$ - see front matter
PII: S0009-2614(02)00835-7

HO–H–Cl angle quite close to 180°. The symmetry of the system is not fully reproduced by the CNH functional since the two hydrogen atoms are unevenly dealt. Reaction coefficients were calculated on the CNH PES using a reduced dimensionality RBA quantum approach [10]. The far too small value of the calculated rates motivated the authors of [8] to lower the energy of the transition state (TS) to 0.25 kcal mol^{-1}.

In 1997, Steckler and coworkers performed an ab initio direct dynamics calculation of the rate coefficients of the OH + HCl reaction using a technique based on the transition state theory and concentrated their efforts on the accurate determination of the minimum energy path (MEP) around the transition state [11]. This PES (STWB), whose geometries were optimized using the MBPT(2)/DZP method and whose energies were calculated using the CCSD(T)/PVQZ technique, has a not coplanar transition state (the torsion angle is 59°). It has a *cis* configuration and a clearly more bent shape (it deviates from collinearity of 37° with respect to the 13° of the CNH PES). The CNH and the STWB surfaces differ also for the height of the transition state (that is 2.43 kcal mol^{-1} for the STWB PES) and for the slope of the MEP around the transition state (this is less sudden for the STWB PES).

Finally, in the year 2000, Yu and Nyman [12] published a PES (YN) based on the interpolation of new ab initio potential energy values. The height of the transition state is 2.06 kcal mol^{-1} and the geometry of the transition state almost coincides with that of the STWB PES. However, to enhance the reactivity of the YN PES, an additional empirical correction of the height of the barrier to reaction (from 2.06 kcal mol^{-1} to the estimated value of 0.89 kcal mol^{-1}) was introduced by the authors.

In this Letter we use the Largest Angle Generalization of the ROtating Bond Order (LAGROBO) functional obtained from an extension to four atom systems [13,14] of the three atom rotating diatomic-like bond order model (ROBO) [15–18] defined in the hyperspherical representation of the bond order space [19]. The particular flexibility of the LAGROBO functional has allowed us to optimize the height of the barrier to reaction of the OH + HCl system to the reproduction of the measured rate coefficients by means of quasiclassical trajectory calculations performed using a modified version of the VENUS program [14,20].

The Letter is organized as follows: In Section 2 the details of the proposed LAGROBO PESs are illustrated; In Section 3 the calculated rate coefficients are compared with the experimental data.

2. The LAGROBO PESs

The LAGROBO functional is based on a proper combination of rotating diatomic-like bond order formulations of single process interactions [15,17,18]. Accordingly, the overall potential V of a tetratomic (κ, λ, μ, ν) system is expressed as a combination of 12 individual process contributions V^P [13]

$$V = \frac{\sum_P w^P V^P}{\sum_P w^P} \tag{1}$$

through a weight w^P that allows a proper switching from one V^P to another.

The individual process term, V^P, is formulated as a rotating bond order model potential. To this end the process interaction is expressed as

$$V^P = D^P F^P + I^P, \tag{2}$$

where $D^P F^P$ is a diatomic-like potential with D^P being the dissociation energy and F^P a polynomial in the hyperradius ρ of the bond order (BO) hyperspace (the bond order space associated with the bond order coordinates [1] of the arrangement chosen to describe the process). I^P is a corrective term accounting for the interaction that cannot be reconducted to the $D^P F^P$ term of the diatoms explicitly considered by process P.

The V^P terms and related weights w^P are formulated in a way that makes it easier to link them to measured and calculated properties of the as-

[1] The bond order coordinate for the generic $\kappa\lambda$ diatom is $n_{\kappa\lambda} = \exp[-\beta_{\kappa\lambda}(r_{\kappa\lambda} - r_{e\kappa\lambda})]$.

ymptotic fragments and to the characteristics of the saddle to reaction of the potential energy surface. However, the symmetry of the system, reduces the number of processes needed to describe the OH + HCl reaction from 12 to the following 6 ones:

$$H + OHCl \rightleftharpoons HO + HCl \rightleftharpoons HOH + Cl$$

$$H + OClH \rightleftharpoons HO + ClH \rightleftharpoons HOCl + H$$

$$H + HOCl \rightleftharpoons HH + OCl \rightleftharpoons HHO + Cl$$

$$H + HClO \rightleftharpoons HH + ClO \rightleftharpoons HHCl + O$$

$$H + ClHO \rightleftharpoons HCl + HO \rightleftharpoons HClH + O$$

$$O + HHCl \rightleftharpoons OH + HCl \rightleftharpoons OHH + Cl$$

Moreover, the energetics of the reaction is such that only the $OH + HCl \rightleftharpoons Cl + H_2O$ process can take place at the (fairly low) energies of the experiment.

The V^P term of the OH + HCl process was, as usual, built by incorporating the available experimental and theoretical information. This means that, to shape the asymptotes and enforce the reproduction of the energetic balance of the process, use was made of spectroscopic data [21–23]. Accordingly, the following values of the Morse potential parameters were used: $r_e = 0.9697$ Å, $D_e = 106.45$ kcal mol^{-1} and $\beta = 2.296$ Å^{-1} for OH, $r_e = 1.2746$ Å, $D_e = 106.36$ kcal mol^{-1}, and $\beta = 1.868$ Å^{-1} for HCl. The values of the parameters adopted for the triatomic H_2O molecule are the same as those given in [13] for the OH_3 LAGROBO surface.

Far from the asymptotes the V^P term is characterized by the location of the reaction channel energy minimum, ρ_0, and by the related energy value, D. A proper choice of ρ_0 and D ensures a smooth interconnection of the various atom + atom + diatom, diatom + diatom, atom + triatom asymptotes and the reproduction of the critical features of the strong interaction region. In the LAGROBO functional ρ_0 and D depend directly upon the angles α and σ and parametrically upon the angles τ, δ and γ which are functions of the angles ϕ, ψ and θ characterizing the geometry of the system [2].

To shape the PES, one first draws the fixed τ, δ and γ minimum energy paths of the $\alpha\sigma$ planes using the ab initio potential energy values. Then, the values of $\rho_0(\alpha, \sigma; \tau, \delta, \gamma)$ and $D(\alpha, \sigma; \tau, \delta, \gamma)$ at the asymptotes and at the saddle to reaction are interpolated using a trigonometric function. This ensures that all the minimum energy paths reproduce not only the asymptotes but also the location and the height of the related barrier to reaction. In the next step the variation of the characteristics of the barrier to reaction with the angles τ, δ and γ (that is, as a function of the relative orientation of the system) is formulated. To this end, one first singles out the dependence of the value of ρ_0 and D at the saddle to reaction TS ($\rho_{0TS}(\tau; \delta, \gamma)$ and $D_{TS}(\tau; \delta, \gamma)$, respectively) on the angle τ that is a measure of the collinearity of the system. The same approach is adopted for $\alpha_{TS}(\tau; \delta, \gamma)$ and $\sigma_{TS}(\tau; \delta, \gamma)$ (the value of α and σ at the TS) to single out their dependence on τ.

To define the dependence of the $\rho_{0TS}(\tau; \delta, \gamma)$, $D_{TS}(\tau; \delta, \gamma)$, $\alpha_{TS}(\tau; \delta, \gamma)$ and $\sigma_{TS}(\tau; \delta, \gamma)$ on τ, their values were calculated at $\tau = 0$, $\tau = \tau_1 > 0$, and $\tau = \tau_2 > \tau_1$ and then interpolated using a second order polynomial. The value of these functions at $\tau = 0$ (the linear geometry) is independent of δ and γ while it depends on them at τ_1 and τ_2. Such a dependence is rendered in terms of a Fourier series in γ whose coefficients are polynomials in δ. As an example, for ρ_{0TS} and D_{TS} at $\tau = \tau_1$ it reads

$$D_{TS,\tau_1}(\gamma; \delta) = \frac{c_0^{(6)}(\delta)}{2} + \sum_{l=2,4,6,8} [c_{l-1}^{(6)}(\delta)\sin(l\gamma) + c_l^{(6)}(\delta)\cos(l\gamma)],$$

[2] The angles α and σ are defined as

$$\rho = \sqrt{n_{\kappa\lambda}^2 + n_{\lambda\mu}^2 + n_{\mu\nu}^2}, \quad \alpha = \arctan\left(\frac{n_{\mu\nu}}{n_{\kappa\lambda}}\right), \quad \sigma = \arccos\left(\frac{n_{\lambda\mu}}{\rho}\right),$$

(see [13]) while the angles τ, δ and γ are defined as

$$\tau = \sqrt{\phi'^2 + \psi'^2 + \theta'^2}, \quad \delta = \arctan\left(\frac{\psi'}{\theta'}\right), \quad \gamma = \arccos\left(\frac{\phi'}{\tau}\right),$$

with

$$\phi' = 2\pi - 2\phi, \quad \psi' = 2\psi - 2\pi, \quad \theta' = 4\theta.$$

$$\rho_{0\mathrm{TS},\tau_1}(\gamma;\delta) = \frac{c_0^{(10)}(\delta)}{2} + \sum_{l=2,4,6,8} [c_{l-1}^{(10)}(\delta)\sin(l\gamma) + c_l^{(10)}(\delta)\cos(l\gamma)], \quad (3)$$

where the c coefficients are further expressed as

$$c_i^{(6)}(\delta) = \sum_{j=0}^{6} c_{ij}^{(5)}\delta^j, \qquad c_i^{(10)}(\delta) = \sum_{j=0}^{6} c_{ij}^{(9)}\delta^j. \quad (4)$$

We proceeded in the same way for $\alpha_{\mathrm{TS},\tau_1}(\delta,\gamma)$ and $\sigma_{\mathrm{TS},\tau_1}(\delta,\gamma)$. Related coefficients are $c^{(13)}$ and $c^{(14)}$ for $\alpha_{\mathrm{TS},\tau_1}$ and $c^{(17)}$ and $c^{(18)}$ for $\sigma_{\mathrm{TS},\tau_1}$. A similar approach was followed also at $\tau = \tau_2$ using the coefficients $c^{(7)}$ and $c^{(8)}$ for $D_{\mathrm{TS},\tau_2}(\gamma,\delta)$, $c^{(11)}$ and $c^{(12)}$ for $\rho_{0\mathrm{TS},\tau_2}(\gamma,\delta)$, $c^{(15)}$ and $c^{(16)}$ for $\alpha_{\mathrm{TS},\tau_2}(\delta,\gamma)$ and $c^{(19)}$ and $c^{(20)}$ for $\sigma_{\mathrm{TS},\tau_2}(\delta,\gamma)$. The values of all these coefficients are given in Tables 1 and 2 for τ_1 and τ_2, respectively. Please notice that the $c_{00}^{(5)}$ coefficient gives the height of the transition state of the OH + HCl reaction. At $\tau = 0$ the values of D, ρ_0, α and σ are 29.867 kcal mol^{-1}, 1.404, 0.403 and 0.953, respectively.

Using the LAGROBO functional form we have generated three PESs (LGR1, LGR2 and LGR3). The three PESs have the same reactant and product asymptotes and a similar transition state. They differ almost exclusively for the height of the transition state and, accordingly, for the description of the nearby strong interaction region. As already mentioned, the procedure for tuning the height of the saddle to reaction is simple since it consists in adjusting the value of $c_{00}^{(5)}$ (see Table 1). We first developed the LAGROBO PES LGR1 that has a barrier to reaction of 2.28 kcal mol^{-1} (a value close to that of the ab initio data) and makes the calculations underestimate the reaction coefficients. Because of this we built another PES (LGR2) having a TS energy close to that of the CNH PES [8] and the LGR3 surface having a TS energy of 1.00 kcal mol^{-1} (a value intermediate between that of LGR1 and LGR2).

3. Calculated dynamical properties

On the LGR1, LGR2 and LGR3 PESs we have calculated the rate coefficients at a set of temperatures spanning the range covered by the experiment (138–1055 K).

The details of the quasiclassical trajectory calculation are as follows: The derivatives of the LAGROBO surfaces were performed numerically. The time step used for the integration was 0.05 fs and the error made in the evaluation of the total energy was of the order of 10^{-3} kcal mol^{-1}. This led to an acceptable compromise between numerical accuracy and time required to integrate a set of trajectories that varies, for example, on the LGR3 PES from 4200 (at $T = 1055$ K) to 18 000 (at $T = 298$ K). The maximum value of the impact parameter used for the integration also depends on the temperature. It varies from 4.0 Å (at $T = 138$ K) to 2.80 Å (at $T = 1055$ K). In all cases the sample of trajectories integrated was large enough to guarantee a statistical error smaller than 15%. The initial and final collision distances were set at 7 Å. The resulting typical collision time of a reactive trajectory is 1 ps.

The values of the rate coefficient calculated on the LAGROBO PESs are compared in Fig. 1 with experimental data. Theoretical values calculated on the LGR1 PES are very small and are not shown in the figure. Their contribution to the investigation consists mainly in confirming the need for lowering the height of the ab initio barrier to reaction as indicated also by previous theoretical work [8,12]. Rate coefficients calculated on the LGR2 and on the LGR3 PESs are instead plotted in Fig. 1 as solid diamonds and solid squares, respectively.

For comparison, following the IUPAC recommendation [7] for the overall temperature range, we also plot as a solid line the three parameter Arrhenius curve $k = 3.28 \times 10^{-17} T^{1.66} \exp[184/T]$ cm^3 s^{-1} given in [6]. In the same figure we plot also as open circles the low temperature values of [5]. As apparent from the figure, the LGR2 and LGR3 results are quite different. In fact, they lie quite close to the experimental curve at the two highest temperatures (with those of LGR2 slightly closer to the experiment than those of LGR3). As temperature decreases, while the rate coefficients calculated on LGR3 remain close to the experimental values (especially if results of [5] are taken into account) those calculated on LGR2 progressively deviate from the experimental data to become three times larger at the lowest temperature considered.

Table 1
Coefficients of the expansion of D_{TS}, ρ_{0TS}, α_{TS} and σ_{TS} at $\tau = \tau_1$

	j	i						
		0	1	2	3	4	5	6
$c_{ij}^{(5)}$	0	−3.936(+2)	3.294(+0)	2.093(+1)	3.138(+0)	1.944(+0)	−5.865(−1)	−8.508(−1)
	1	−9.255(+0)	1.886(+0)	−6.633(+0)	−2.763(+0)	−1.128(+0)	5.165(−1)	3.911(−1)
	2	−1.326(+1)	7.114(−2)	−4.793(+0)	3.579(−2)	−1.582(+0)	−6.690(−3)	4.646(−1)
	3	4.986(+0)	−6.208(−1)	−1.045(+0)	−7.098(−1)	6.395(−1)	1.326(−1)	−1.323(−1)
	4	3.366(+0)	−1.919(+0)	−6.767(+0)	−1.776(+0)	5.340(−1)	3.319(−1)	−8.354(−4)
	5	−1.313(+0)	7.737(−1)	2.823(+0)	7.484(−1)	−2.108(−1)	−1.398(−1)	−2.493(−3)
	6	1.239(+0)	−6.954(−2)	1.461(−1)	−7.708(−2)	1.525(−1)	1.440(−2)	−3.891(−2)
	7	−2.881(−1)	6.969(−2)	2.225(−1)	8.066(−2)	−3.949(−2)	−1.507(−2)	5.233(−3)
	8	−4.878(−1)	2.765(−1)	9.685(−1)	2.536(−1)	−7.722(−2)	−4.741(−2)	3.109(−4)
$c_{ij}^{(9)}$	0	2.645(+0)	9.232(−2)	−1.911(−1)	−7.396(−2)	5.830(−2)	1.382(−2)	−1.027(−2)
	1	6.063(−3)	−9.050(−2)	6.616(−2)	6.357(−2)	−2.975(−2)	−1.188(−2)	5.828(−3)
	2	−8.355(−3)	2.529(−3)	6.203(−2)	−1.992(−3)	−1.613(−2)	3.724(−4)	2.675(−3)
	3	5.746(−3)	−2.214(−2)	−2.369(−3)	1.744(−2)	−1.413(−3)	−3.259(−3)	3.794(−4)
	4	8.595(−3)	−5.371(−2)	4.311(−2)	4.303(−2)	−1.595(−2)	−8.043(−3)	2.983(−3)
	5	−3.568(−3)	2.268(−2)	−1.816(−2)	−1.811(−2)	6.758(−3)	3.384(−3)	−1.265(−3)
	6	1.056(−3)	−2.479(−3)	−3.574(−3)	1.953(−3)	7.150(−4)	−3.651(−4)	−1.031(−4)
	7	−4.803(−4)	2.485(−3)	−1.055(−3)	−1.958(−3)	5.074(−4)	3.659(−4)	−1.007(−4)
	8	−1.231(−3)	7.668(−3)	−6.158(−3)	−6.148(−3)	2.276(−3)	1.149(−3)	−4.255(−4)
$c_{ij}^{(13)}$	0	1.207(+0)	7.537(−2)	−1.216(−1)	−5.405(−2)	5.068(−4)	1.010(−2)	2.142(−3)
	1	2.918(−2)	−7.428(−2)	4.281(−2)	4.905(−2)	−5.386(−3)	−9.167(−3)	4.818(−4)
	2	5.269(−2)	2.066(−3)	1.915(−2)	−1.466(−3)	1.406(−2)	2.740(−4)	−3.693(−3)
	3	−1.727(−2)	−1.809(−2)	1.196(−2)	1.283(−2)	−9.566(−3)	−2.398(−3)	2.047(−3)
	4	−5.282(−3)	−4.385(−2)	4.819(−2)	3.145(−2)	−1.460(−2)	−5.877(−3)	2.570(−3)
	5	1.954(−3)	1.852(−2)	−2.007(−2)	−1.325(−2)	6.030(−3)	2.477(−3)	−1.057(−3)
	6	−4.652(−3)	−2.026(−3)	2.405(−4)	1.437(−3)	−1.766(−3)	−2.686(−4)	4.147(−4)
	7	8.537(−4)	2.030(−3)	−1.782(−3)	−1.440(−3)	7.964(−4)	2.692(−4)	−1.558(−4)
	8	7.727(−4)	6.260(−3)	−6.898(−3)	−4.491(−3)	2.095(−3)	8.395(−4)	−3.687(−4)
$c_{ij}^{(17)}$	0	2.269(+0)	−4.625(−2)	1.405(−1)	4.255(−2)	−6.269(−2)	−7.953(−3)	1.226(−2)
	1	2.125(−2)	3.314(−2)	−4.272(−2)	−2.791(−2)	2.563(−2)	5.216(−3)	−5.288(−3)
	2	6.189(−2)	−1.221(−3)	−6.671(−2)	1.113(−3)	2.724(−2)	−2.081(−4)	−5.224(−3)
	3	−2.615(−2)	1.068(−2)	1.589(−2)	−9.749(−3)	−5.220(−3)	1.822(−3)	9.431(−4)
	4	−2.207(−2)	2.691(−2)	−1.017(−2)	−2.476(−2)	7.087(−3)	4.629(−3)	−1.492(−3)
	5	8.898(−3)	−1.127(−2)	4.484(−3)	1.036(−2)	−3.092(−3)	−1.936(−3)	6.503(−4)
	6	−6.086(−3)	1.197(−3)	5.257(−3)	−1.091(−3)	−2.012(−3)	2.040(−4)	3.798(−4)
	7	1.675(−3)	−1.200(−3)	−3.951(−4)	1.094(−3)	1.579(−5)	−2.045(−4)	3.602(−6)
	8	3.179(−3)	−3.848(−3)	1.440(−3)	3.542(−3)	−1.005(−3)	−6.621(−4)	2.116(−4)

The meaning of the coefficients is explained in the text.

To give a quantitative estimate of the accuracy of the calculated rate coefficients we evaluated the root mean square percentual deviation of calculated values from recommended IUPAC ones. These values are 108% for LGR2 and 22% for LGR3 and indicate that the LGR3 PES is quite accurate (even more accurate if one refers to the experimental values of [5]) and, in any case, of the order of the statistical error associated with the trajectory integration procedure.

Obviously, the conclusions drawn here are to be taken with caution. The value of the calculated rate coefficients, in fact, clearly depends on the functional used to formulate the PES and on the method used for perform the dynamic treatment. As an example, it is well known that trajectory calculations are increasingly less reliable when the

Table 2
Coefficients of the expansion of D_{TS}, ρ_{0TS}, α_{TS} and σ_{TS} at $\tau = \tau_2$

	j	i						
		0	1	2	3	4	5	6
$c_{ij}^{(7)}$	0	−3.348(+02)	−5.671(−01)	1.443(+02)	−2.006(−09)	−2.134(+01)	6.054(−10)	2.380(+00)
	1	−3.629(+01)	−3.550(+00)	−3.771(+01)	1.734(−09)	5.577(+00)	−5.233(−10)	−6.220(−01)
	2	1.355(+01)	1.377(−05)	−8.227(+01)	1.918(−11)	1.216(+01)	−5.630(−12)	−1.357(+00)
	3	−4.219(+00)	1.509(−06)	2.560(+01)	−2.341(−11)	−3.786(+00)	6.824(−12)	4.222(−01)
	4	3.397(+00)	3.323(−01)	3.530(+00)	1.108(−09)	−5.220(−01)	−3.343(−10)	5.822(−02)
	5	−1.130(+00)	−1.105(−01)	−1.174(+00)	−4.852(−10)	1.736(−01)	1.464(−10)	−1.936(−02)
	6	−1.173(+00)	6.086(−07)	7.120(+00)	−1.630(−11)	−1.053(+00)	4.754(−12)	1.174(−01)
	7	1.938(−01)	−5.330(−07)	−1.176(+00)	5.838(−12)	1.739(−01)	−1.704(−12)	−1.939(−02)
	8	−5.055(−01)	−4.945(−02)	−5.252(−01)	−1.165(−10)	7.768(−02)	3.517(−11)	−8.663(−03)
$c_{ij}^{(11)}$	0	2.417(+00)	1.010(−03)	−1.194(−01)	−2.321(−11)	1.767(−02)	6.493(−12)	−1.970(−03)
	1	6.982(−02)	6.327(−03)	−5.707(−02)	2.011(−11)	8.440(−03)	−5.625(−12)	−9.413(−04)
	2	−9.281(−02)	−2.454(−08)	6.039(−02)	−7.383(−14)	−8.932(−03)	1.579(−14)	9.960(−04)
	3	2.888(−02)	−2.689(−09)	−1.879(−02)	9.606(−14)	2.779(−03)	−2.040(−14)	−3.099(−04)
	4	−6.535(−03)	−5.922(−04)	5.342(−03)	1.284(−11)	−7.900(−04)	−3.593(−12)	8.810(−05)
	5	2.174(−03)	1.970(−04)	−1.777(−03)	−5.628(−12)	2.628(−04)	1.574(−12)	−2.931(−05)
	6	8.032(−03)	−1.084(−09)	−5.226(−03)	6.670(−14)	7.729(−04)	−1.415(−14)	−8.619(−05)
	7	−1.326(−03)	9.498(−10)	8.633(−04)	−2.358(−14)	−1.276(−04)	4.953(−15)	1.423(−05)
	8	9.724(−04)	8.813(−05)	−7.949(−04)	−1.352(−12)	1.175(−04)	3.785(−13)	−1.311(−05)
$c_{ij}^{(15)}$	0	9.530(−01)	6.055(−03)	−7.685(−02)	−4.232(−12)	1.136(−02)	1.863(−12)	−1.267(−03)
	1	1.354(−01)	3.791(−02)	−1.175(−01)	3.683(−12)	1.738(−02)	−1.619(−12)	−1.938(−03)
	2	−8.251(−02)	−1.470(−07)	3.177(−02)	−4.968(−15)	−4.699(−03)	1.908(−15)	5.241(−04)
	3	2.567(−02)	−1.611(−08)	−9.888(−03)	5.847(−15)	1.462(−03)	−2.292(−15)	−1.630(−04)
	4	−1.268(−02)	−3.548(−03)	1.100(−02)	2.350(−12)	−1.627(−03)	−1.034(−12)	1.814(−04)
	5	4.218(−03)	1.180(−03)	−3.660(−03)	−1.029(−12)	5.413(−04)	4.530(−13)	−6.036(−05)
	6	7.140(−03)	−6.498(−09)	−2.749(−03)	3.953(−15)	4.067(−04)	−1.559(−15)	−4.535(−05)
	7	−1.179(−03)	5.690(−09)	4.542(−04)	−1.329(−15)	−6.718(−05)	5.334(−16)	7.492(−06)
	8	1.887(−03)	5.280(−04)	−1.637(−03)	−2.474(−13)	2.421(−04)	1.088(−13)	−2.700(−05)
$c_{ij}^{(19)}$	0	2.141(+00)	−2.144(−03)	3.855(−02)	1.725(−11)	−5.702(−03)	−1.971(−12)	6.359(−04)
	1	1.105(−01)	−1.342(−02)	7.287(−02)	−1.494(−11)	−1.077(−02)	1.705(−12)	1.201(−03)
	2	−6.707(−02)	5.208(−08)	−1.472(−02)	−2.674(−14)	2.178(−03)	1.752(−14)	−2.429(−04)
	3	2.087(−02)	5.707(−09)	4.583(−03)	3.372(−14)	−6.778(−04)	−2.259(−14)	7.559(−05)
	4	−1.034(−02)	1.256(−03)	−6.820(−03)	−9.549(−12)	1.008(−03)	1.090(−12)	−1.124(−04)
	5	3.443(−03)	−4.180(−04)	2.269(−03)	4.182(−12)	−3.355(−04)	−4.780(−13)	3.742(−05)
	6	5.804(−03)	2.301(−09)	1.274(−03)	2.350(−14)	−1.885(−04)	−1.575(−14)	2.102(−05)
	7	−9.588(−04)	−2.015(−09)	−2.105(−04)	−8.248(−15)	3.113(−05)	5.595(−15)	−3.472(−06)
	8	1.540(−03)	−1.870(−04)	1.014(−03)	1.004(−12)	−1.501(−04)	−1.150(−13)	1.673(−05)

The meaning of the coefficients is explained in the text.

temperature (or the energy) decreases. Unfortunately, a comparison with exact quantum calculations is still prohibitive. For this reason, to investigate the role played by quantum effects and to understand the low temperature behaviour of rate coefficients we repeated the calculations using, as in [6,11], the improved canonical variational transition state with small curvature tunneling corrections (ICVT/SCT) method as implemented in the POLYRATE package [24]. As shown in Fig. 2, where ICVT/SCT results calculated for LGR1 (long dashed line), LGR2 (short dashed line), and LGR3 (dashed dotted line) are plotted, ICVT/SCT results increasingly underestimate both experimental and trajectory results as temperature decreases. The fact that ICVT/SCT results become increasingly smaller than quasiclassical and measured data as temperature lowers, implies that the

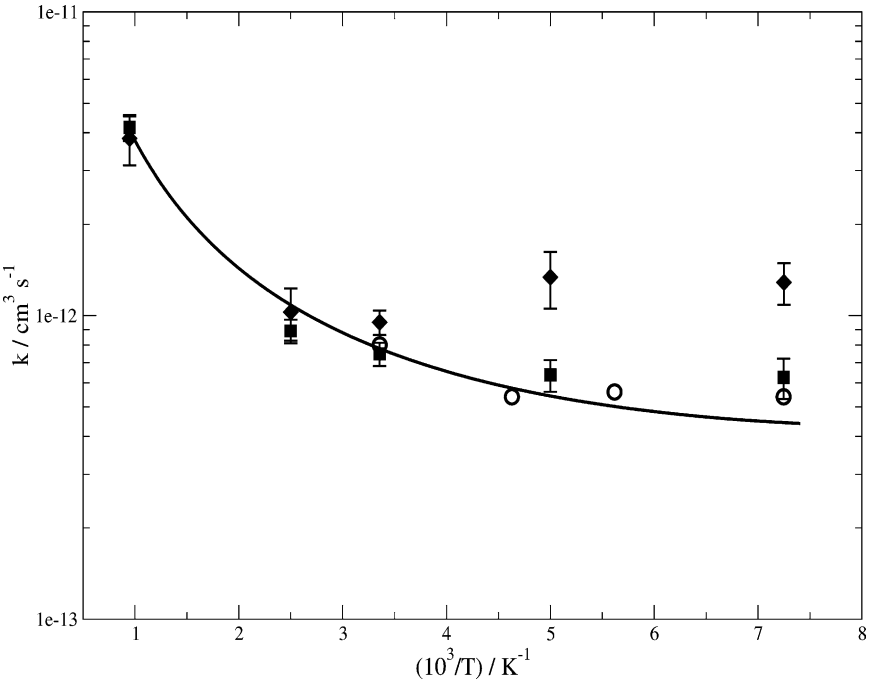

Fig. 1. Quasiclassical reaction rate coefficients calculated on the LGR2 (solid diamonds) and LGR3 (solid squares) PESs plotted as a function of the inverse temperature. For comparison also experimental values of [5] (open circles) and [6] (solid line) are shown.

adoption of reduced dimensionality approaches sacrifices a large fraction of collisions that a proper dynamical treatment would drive into the product channel despite the fact that the inclusion of tunneling effects enhances the reactivity. This implies that the rate coefficients calculated on the STWB PES [6,11] using POLYRATE (and shown in the same figure as a dotted line and plus symbols) could also be much lower than corresponding full dimensional trajectory results calculated on the same surface and therefore lead to a worse agreement with the experiment.

To a certain extent this could also have affected the values of the rate coefficients given in [8,12] (see stars and crosses of Fig. 2) calculated using a reduced dimensionality quantum method (although this statement cannot be put on a quantitative basis on the ground of a comparison with the ICVT/SCT calculations). It is also worth noticing, however, that both RBA results give a temperature dependence of the reaction coefficients less negative than the extrapolated ones and closer to that of measurements of [5]. At low temperature, also the LGR3 results show a temperature dependence that agrees with that of the measurements of [5].

All these considerations suggest that the LGR3 PES is a good basis for starting an iterative procedure aimed at developing an accurate PES for the OH + HCl reaction based on exact quantum calculations and a multiproperty analysis.

4. Conclusions

In this Letter the LAGROBO formulation of the four atom interaction for reactive systems has been revisited and applied to the OH + HCl reaction. Thanks to the fact that the parameters of the LAGROBO PES can be tuned to allow the reproduction of the spectroscopic properties of the fragments and of the measured rate coefficients we have built three potential energy surfaces having a different height of the barrier to reaction.

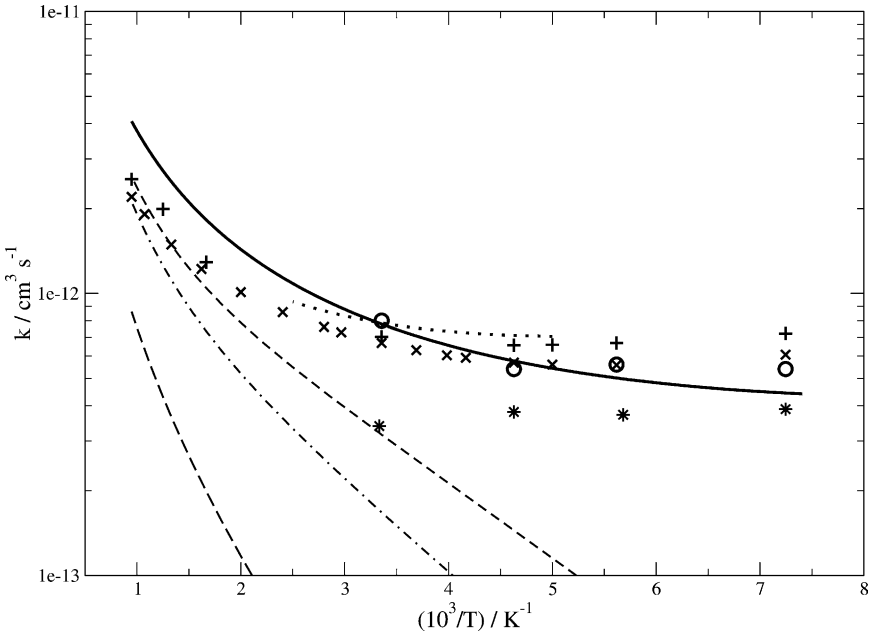

Fig. 2. ICVT/SCT reaction rate coefficients calculated on the LGR1 (long dashed line), LGR2 (short dashed line), LGR3 (dashed dotted line) PESs. For comparison also experimental values of [5] (open circles) and [6] (solid line) and values obtained from previous theoretical investigations performed on the STWB (dotted line [6] and plus symbols [11]), CNH (stars [8]) and YN (crosses [12]) PESs are shown.

Then we have calculated the quasiclassical estimates of the rate coefficients and their dependence on the temperature. This has allowed us to single out a LAGROBO potential energy surface (LGR3) that has a root mean square percentual deviation between calculated and measured rate coefficient values of the order of the statistical error associated with the trajectory integration procedure. This credits LGR3 as a suitable basis for an iterative multiproperty analysis based upon accurate dynamical calculations. This will allow us to spot possible conditionings associated with the LAGROBO functional form and the limitations of quasiclassical trajectory treatments. Work along this direction is already in progress.

Acknowledgements

Partial financial support from the MEC (PB98-0281), from MURST, ASI and CNR is acknowledged. This work has been carried out as a part of the COST in Chemistry European Cooperative Project D23/003/01.

References

[1] M.J. Molina, L.T. Molina, C.A. Smith, Int. J. Chem. Kinet. 16 (1984) 1151.
[2] L.F. Keyser, J. Phys. Chem. 88 (1984) 4750.
[3] D. Husain, J.M.C. Plane, C.C. Xiang, J. Chem. Soc. Faraday Trans. 2 (80) (1984) 713.
[4] A.R. Ravishankara, P. Wine, J.R. Wells, R.L. Thompson, Int. J. Chem. Kinet. 17 (1985) 1281.
[5] P. Sharkey, I.W.M. Smith, J. Chem. Soc. Faraday Trans. 2 89 (1993) 631.
[6] F. Battin-Leclerc, I.K. Kim, R.K. Talukdar, R.W. Portmann, A.R. Ravishankara, R. Steckler, D. Brown, J. Phys. Chem. A 103 (1999) 3237.
[7] R. Atkinson, D.L. Baulch, R.A. Cox, R.F. Hampson Jr., J.A. Kerr, M.J. Rossi, J. Troe, J. Phys. Chem. Ref. Data 29 (2000) 167.
[8] D.C. Clary, G. Nyman, R. Hernandez, J. Chem. Phys. 101 (1994) 3704.
[9] J.N. Murrell, S. Carter, J. Phys. Chem. 21 (1984) 4887.

[10] D.C. Clary, J. Chem. Phys. 95 (1991) 7298.
[11] R. Steckler, G.M. Thurman, J.D. Watts, R.J. Bartlett, J. Chem. Phys. 106 (1997) 3926.
[12] H.-G. Yu, G. Nyman, J. Chem. Phys. 113 (2000) 8996.
[13] G. Ochoa de Aspuru, D.C. Clary, J. Phys. Chem. A 102 (1998) 9631.
[14] A. Rodriguez, Ph.D. Thesis, Universidad del País Vasco, 2001.
[15] A. Laganà, J. Chem. Phys. 95 (1991) 2216.
[16] A. Laganà, G. Ferraro, E. Garcia, O. Gervasi, A. Ottavi, Chem. Phys. 168 (1992) 341.
[17] E. Garcia, A. Laganà, J. Chem. Phys. 103 (1995) 5410.
[18] A. Laganà, G. Ochoa de Aspuru, E. Garcia, J. Chem. Phys. 108 (1998) 3886.
[19] A. Laganà, N. Faginas Lago, A. Riganelli, G. Ferraro, in: XIX International Conference on Molecular Beams, June 2001.
[20] W.H. Hase, R.J. Duchovic, X. Hu, K.F. Lim, D.-H. Lu, G.H. Peslherbe, K.N. Swamy, S.R. Van de Linde, H. Wang, R.J. Wolf, Quantum Chem. Program Exchange Bull. 16 (1996) 671.
[21] G. Herzberg, in: Molecular Spectra and Molecular Structure. I. Spectra of Diatomic Molecules, second edn., Van Nostrand Reinhold, New York, 1950.
[22] G. Herzberg, in: Molecular Spectra and Molecular Structure. II. Infrared and Raman Spectra of Polyatomic Molecules, Van Nostrand Reinhold, New York, 1945.
[23] K.P. Huber, G. Herzberg, in: Molecular Spectra and Molecular Structure. IV. Constants of Diatomic Molecules, Van Nostrand Reinhold, New York, 1979.
[24] R. Steckler, W.-P. Hu, Y.-P. Liu, G.C. Lynch, B.C. Garrett, A.D. Isaacson, D.-H. Lu, V.S. Melissas, T.N. Truong, S.N. Rai, G.C. Hancock, J.G. Lauderdale, T. Joseph, D.G. Truhlar, Quantum Chem. Program Exchange Bull. 15 (1995) 32.